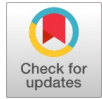# Predictive Controller Strategies for Electrical Drives System using Inverter System

Suraj R. Karpe, S. A. Deokar, U. B. Shinde

*Abstract: Advanced control strategies in power electronics include Predictive controller of current (P CURRENT CONTROL) and Predictive controller of torque (P TORQUE CONTROL). In order to operate a SRM or an induction machine, the Predictive controller of torque (P TORQUE CONTROL) approach analyses the stator flux and electromagnetic torque in the cost function (IM), and the Predictive controller of current (P CURRENT CONTROL) method [1,2] takes errors between the current reference and the measured current into account in the cost function. The switching vector selected for usage in IGBTs reduces the error between the references and the predicted values. The system restrictions are easy to include [4, 5]. The weighting component is not required. Together with the P TORQUE CONTROL and P CURRENT CONTROL systems, the SRM method is the most practicable direct control technique since it doesn't require a modulator and offers 10% to 30% more power than an induction motor [3]. With the same current, an induction motor can only generate between 70 and 90 percent of the force generated by an SRM due to its lagging power factor. SRM approach decreases 23% more THD in torque, speed, and stator current when P CURRENT CONTROL and P TORQUE CONTROL method with 15-level H-bridge multilevel inverter is compared to P CURRENT CONTROL and P TORQUE CONTROL method with 15-level H-bridge multilevel inverter utilising induction motor [21]. The transistors are only swapped when necessary to maintain the limits of torque and flux, which minimises switching losses. To improve the efficiency of a multilevel inverter, semiconductor switches are switched in a specific pattern. In contrast to the P TORQUE CONTROL and P CURRENT CONTROL approaches using a 2-level voltage source inverter, the 15-level H-bridge multilevel inverter employed in this study, coupled with SRM and IM, gives outstanding torque and flux responses and achieves robust and stable operation. This unique strategy quickly caught the interest of academics due to its simple algorithm and high performances in both steady and transient modes [8].*

*Keywords: Voltage Source Inverter, Predictive Controller of current (P CURRENT CONTROL), Predictive Controller of Torque (P TORQUE CONTROL), Synchronous Reluctance Motor (SRM), Electrical Motors, 15-level H-Bridge Inverter*

*\*Correspondence Author(s)*

**Dr. Suraj R. Karpe**\*, Associate Professor, Department of Electrical Engineering CSMSS Chh. Shahu College of Engineering, Aurangabad (Maharashtra), India. E-mail: surajkarpe007@gmail.com, ORCID ID: 0000-0002-2812-8757

**Sanjay Deokar**, Department of Electrical Engineering CSMSS Chh. Shahu College of Engineering, Aurangabad (Maharashtra), India. E-mail: s_deokar2@rediffmail.com, ORCID ID: 0000-0003-0603-9136

**Dr. Ulhas B. Shinde**, Principal, CSMSS Chh. Shahu College of Engineering, Aurangabad (Maharashtra), India. E-mail: drshindeulhas@gmail.com, ORCID ID: 0009-0005-2424-9841

## I. INTRODUCTION

Predictive controller of current (P CURRENT CONTROL) and Predictive controller of torque are promising methods (P TORQUE CONTROL). The FCS-P TORQUE CONTROL technique shows a number of advantages in addition to reducing torque ripples, such as its ease, straightforwardness, simple implementation, and quick dynamic responses of the algorithm. Calculating the necessary control signals in preparation is the fundamental tenet of the model predictive direct torque control (MPDTC) method [6].

The MPDTC Method does not require pulse width modulation. The control technique requires the inverter type. During MPDTC, the P TORQUE CONTROL and P CURRENT CONTROL method computes all possible voltage vectors, and then selects the best one using an optimum cost function [7]. According to the papers [8] [9], the P CURRENT CONTROL and P TORQUE CONTROL techniques have been extensively studied and

applied in numerous operational contexts to date. Model predictive control (MPC) has attracted considerable consideration and demand in the power electronics systems and industrial machines community in recent years. This MPC control strategy, which was created for process control applications and first introduced in 1970, is extensively used in the sector and has a variety of reported applications [4]. Model predictive control methods' central tenet is that they base choices not on the system's prior state but rather on the anticipated behaviour of the state variables and the proper offline or online selection of the controlled variables. MPC is also known as receding horizon control because its primary function is to continuously slide the prediction horizon in order to represent an endless prediction horizon. The present development and fresh focus in the MPC field described in [5]. The MPC is sometimes used to regulate power converters despite its straightforward design because of its numerical intricacy, which puts a strain on the processors. Due to the development of new, high-speed processors, MPC utilisation has increased today. In [6], a multilayer inverter and VSI are controlled by an MPC, and the VSI's discrete-time model is used to forecast the load current for all potential inverter-generated voltage vectors. According to this, MPC has been extensively used in many power electronics applications, including matrix converters [8] and the management of different industrial drives like DC-DC converters [7].

On the basis of a linearized state-space representation that represents the dynamic operation, MPDTC can also be used to regulate the speed of permanent magnet synchronous motors and induction motors [9] [10] [27] [28].

The P TORQUE CONTROL method has two drawbacks when MPC compares it to the DTC method: rely on speed and require longer computation times. The P TORQUE CONTROL technique takes longer because the optimal cost function is implemented; however, this issue can be readily fixed with improved and faster microprocessing units [10], [11]. In the prediction phases of the conventional P TORQUE CONTROL method for induction machine (IM) and SRM motor applications, the rotor electrical speed is necessary. The estimated speed as well as the observed speed values affect the projected stator current values.

In modern times, connecting a semiconductor switch directly to a system with medium-sized power networks will cause problems. To solve this problem for middle voltage, high voltage, and exceptionally high voltage energy circumstances, a multilevel converter system has been created. A multilevel inverter can use renewable energy as a supply and achieve high power levels. So, for a high power application, green energy sources like solar, fuel cells, and wind can be readily interfaced to a tiered inverter structure. For the past thirty years, the multiple inverter idea has been in use. The multilevel inverter (MLI) has gained a lot of adoration recently and has grown in popularity over time. Because a number of power semiconductor devices and capacitors were used as voltage sources, MLI was able to produce a stepwise voltage pattern with reduced harmonic distortion. The ability of MLI to reduce the voltage burden on power switches, dv/dt ratio, and common mode voltage, thereby improving output quality [12,13], is just one of its many advantages.Diode Clamped Multilevel Inverter, Cascaded Multilevel Inverter, and Flying Capacitor Multilevel Inverter are a few examples of MLI designs. Out of these, the H-Bridge multilevel inverter has a number of benefits, including the ability to operate at lower switching frequencies, generate output voltages with extremely low distortion, draw input current with very low distortion, and generate smaller common-mode (CM) voltage.

In this research, 2-level voltage source inverters are compared to P TORQUE CONTROL and P CURRENT CONTROL techniques with 15-level H-bridge multilevel inverters using SRM and IM. The modelling method was applied to both investigations.When using SRM instead of an induction motor, the P CURRENT CONTROL and P TORQUE CONTROL technique with a 15-level H-bridge multilevel inverter lowers THD by 23% in terms of torque, speed, and stator current [10] [21]. Switching loses reduction through THD minimization is discussed in this article. The transistors are only swapped when necessary to maintain the limits of torque and flux, which minimises switching losses. This novel method quickly caught the interest of academics due to its straightforward formula and powerful findings in both constant and transient states [8,14].

## II. SRM MODELING

Here, the synchronous machine without damper winding model and field current dynamics have been used to develop the mathematical model for the vector control of the SRM. The synchronously revolving rotor reference frame is used to translate stator coil numbers to the synchronous rotating reference frame, which revolves at rotor speed.The SRM without damper winding model that has been built in the rotor reference frame has a sinusoidal induced EMF, limited core losses, and no field current dynamics. The rotor flux is assumed to be constant, concentrated along the d-axis, and negative along the q-axis at a specific working location in the creation of indirect vector controlled induction motor drives. When the location of the rotor magnets is taken into account, it is possible to calculate the immediate induced emf irrespective of the stator voltages and currents, and then the stator currents and torque of the machine.The corresponding q- and d-axis stator windings are converted to the reference frames that revolve at rotor speed when a rotor reference frame is taken into account.The final requirement is that the magnetic fields of the rotor and stator rotate at the same speed and that the windings on the q- and d-axes of the stator are in phase with the rotor magnet axis, which is the d-axis in the design [17,18].

The following describes a complicated equation-based mathematical description of an SRM in the context of a rotor:Voltage equations are given by:

$$V_d = R_s i_d - \omega_r \lambda_q + \frac{d\lambda_d}{dt} \qquad [1]$$

$$V_q = R_s i_q - \omega_r \lambda_d + \frac{d\lambda_q}{dt} \qquad [2]$$

Flux linkage is given by

$$\lambda_q = L_q i_q \qquad [3],$$

$$\lambda_d = L_d i_d + \lambda_f \qquad [4]$$

Substituting Equation 3 and 4 in 1 and 2, we get,

$$V_q = R_s i_q - \omega_r (L_d i_d + \lambda_f) + \frac{d(L_q i_q)}{dt} \qquad [5]$$

$$V_d = R_s i_d - \omega_r L_q i_q. + \frac{d}{dt}(L_d i_d + \lambda_f) \qquad [6]$$

Arranging equation 5 and 6 in matrix form,

$$\begin{pmatrix} V_q \\ V_d \end{pmatrix} = \begin{pmatrix} R_s + \frac{dL_q}{dt} & \omega_r L_d \\ -\omega_r L_q & R_s + \frac{dL_d}{dt} \end{pmatrix} \begin{pmatrix} i_q \\ i_d \end{pmatrix} + \begin{pmatrix} \omega_r \lambda_f \\ \frac{d\lambda_f}{dt} \end{pmatrix} \qquad [7]$$

The developed motor torque is being given by

$$T_e = \frac{3}{2}\left(\frac{P}{2}\right)(\lambda_d i_q - \lambda_q i_d) \qquad [8]$$

$$T_e = \frac{3}{4}P[\lambda_f i_q + (L_d - L_q)i_q i_d] \qquad [9]$$

$$T_e = T_L + B\omega_m + J\frac{d\omega_m}{dt} \qquad [10]$$

Solving for rotor mechanical speed from equation 10, we get,

$$\omega_m = \int \left(\frac{T_e - T_L - B\omega_m}{J}\right) dt \qquad [11]$$

And rotor electrical speed is

$$\omega_r = \omega_m \left(\frac{P}{2}\right) \qquad [12]$$

## III. H-BRIDGE INVERTER

Figure 1 shows an n-level H-bridge cascaded converter in a single-phase arrangement. A single-phase full-bridge/or H-bridge converter is attached to each distinct DC source.

By linking the DC source to the AC output using various configurations of the four switches (S1, S2, S3, and S4), each inverter can produce three distinct voltage levels of output: +Vdc, 0, and -Vdc. Switches S1 and S4 activated for voltage level +Vdc, while S2 and S3 activated for voltage level -Vdc. Switches S1 and S2 or S3 and S4 can be turned on to achieve zero level power. To create the multilayer voltage waveform, the AC outputs of all the synthesised full-bridge inverter levels are linked in series and added together. A cascade inverter has n layers of output phase voltage, where n = 2l+1, where l is the number of independent DC sources. Using (n-1)/2 distinct DC sources and (n- 1)/2 full bridges, a sample phase voltage waveform for an n-level cascaded H-bridge inverter is shown. The output phase voltage generalized use as

$$v = v_{a1} + v_{a2} + v_{a3} + v_{a4} + v_{a5} \dots \dots \dots + v_{an} \qquad [13]$$

he matching stepwise waveform's Fourier transform is as follows [9, 5]:

$$V(\omega t) = \frac{4V_{dc}}{\pi} \sum [\cos(n\theta_1) + \cos(n\theta_2) + \cdots + \cos(n\theta_l)] \frac{\sin(n\omega t)}{n} \qquad [14]$$

where n = 1,3,5,7.

By deciding on conducting angles, 1, 2,..., l, that minimise total harmonic distortion (THD). These propagation angles primarily remove lower frequency harmonics of the fifth, seventh, eleventh, and thirteenth orders in the output [16,19]. The following succinctly summarises the major advantages and disadvantages of cascaded H-bridge multilevel inverters [23]: Benefits: • There are more than twice as many potential output voltage values (n = 2l+1) as there are DC sources.
• The H-bridge line enables modular packing and layout. enable a quicker and more affordable production procedure. Cons: Each H-bridge requires a separate DC source, which may cause fluctuating DC source power.Units
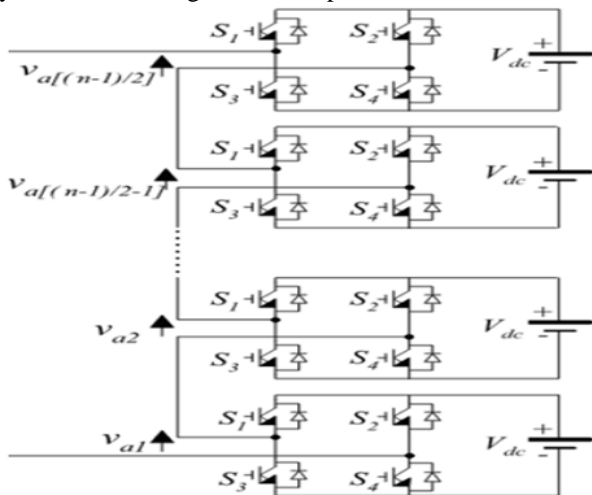


**Fig. 1: Leg of Cascaded H-Bridge Multilevel Structure**

## IV. SWITCHING LOSSES

Transistor losses can be divided into two groups: switching losses (appearing when the devices are switched on or off) and conduction losses. (as a result of ohmic impedance). The commutated current, applied voltage, and semiconductor characteristics all have an impact on these losses. By keeping

in mind that in a VSI inverter, the voltage seen by each semiconductor is always half the total DC-link voltage, the optimal switch turn-on (energy) lost power can be calculated.

$$E_{on} = e_{on} \frac{1}{2} V_{dc} i_{ph} \qquad [15]$$

whereiph is the phase current and aeon is a constant. For the turn-off losses of the perfect switch, an equation with the constant eoff is obtained. Usually, eoff is an order of magnitude larger than aeon. A diode's switch-on losses are virtually nonexistent. The reverse recovery losses, also known as turn-off losses, are erratic in commutated phase current but constant in voltage. Similar to how they do with switching losses, the applied voltage and phase current both have an impact on conduction losses.Despite variations in the neutral point, the DC connection voltage remains consistent. The phase current is the result of adding the fundamental component and the current ripple, and it relies only on the working point—which is determined by the torque and speed—and not on the switching pattern. For a 3-level inverter, the ripple is usually in the region of 10%, which makes it reasonable to assume that conduction losses are unrelated to the switching pattern.

## V. VOLTAGE SOURCE INVERTER

In this study, the P TORQUE CONTROL and P CURRENT CONTROL techniques are also used with a two-level voltage source inverter. Fig. 2 displays the inverter's structure and its practicable voltage vectors. The following vector can be used to represent the transitioning state S:
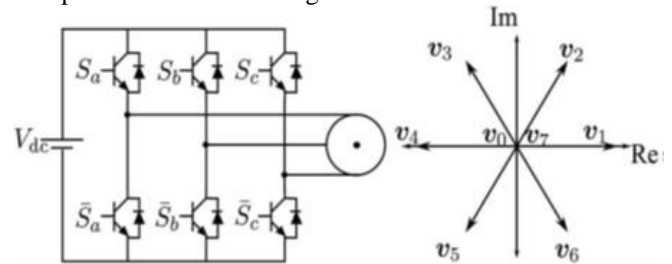


**Fig. 2. Left: Two-Level Voltage Source Inverter; Right: Voltage Vectors**

The eight voltage vectors represented by the stator voltage space vector can be represented as follows by the switching stages and the DC-link voltage, V dc:

$$V_s(S_a, S_b, S_c) = \left(\frac{2}{3}\right) V_{dc} \left(V_a + V_b e^{j\left(\frac{2}{3}\right)} + V_c e^{j\left(\frac{4}{3}\right)}\right) \qquad [16]$$

Where$V_{dc}$, is the DC-link voltage, and the Park's Transformation coefficient of 2/3 is the coefficient. The line-to-line values of the AC motor, which can be written as follows, can be used to obtain the equation:

$$V_{ab} = V_{dc}(S_a - S_b) \qquad [17]$$
$$, V_{bc} = V_{dc}(S_b - S_c) \qquad [18]$$
$$V_{ca} = V_{dc}(S_c - S_a) \qquad [19]$$

The stator phase voltages (line-to-neutral voltages) are required & can be obtained from the line-to-line voltages as.

29

$V_a = (V_{ab} - V_{ca})/3$ [20]

$, V_b = (V_{bc} - V_{ab})/3$ [21]

$, V_c = (V_{ca} - V_{bc})/3$ [22]

If the line-to-line voltages in terms of the DC-link voltage, $V_{dc}$, and switching states aresubstituted into the stator phase voltages it gives:

$V_a = \left(\frac{1}{3}\right) V_{dc}(2S_a - S_b - S_c)$ [23]

$V_b = \left(\frac{1}{3}\right) V_{dc}(-S_a + 2S_b - S_c)$ [24]

$V_a = \left(\frac{1}{3}\right) V_{dc}(-S_a - S_b + 2S_c)$ [25]

The equation can be summarized by combining as:

$V_a = Re(V_s) = \left(\frac{1}{3}\right) V_{dc}(2S_a - S_b - S_c)$ [26]

$V_b = Re(V_s) = \left(\frac{1}{3}\right) V_{dc}(-S_a + 2S_b - S_c)$ [27]

$V_c = Re(V_s) = \left(\frac{1}{3}\right) V_{dc}(-S_a - S_b + 2S_c)$ [28]

$S = \frac{2}{3}(S_a + aS_b + a^2 S_c)$ [29]

where $a = e^{j\frac{2\pi}{3}}$, $S_i = 1$ means $S_i$ON, $\bar{S_i}$means OFF, and$i =$ $a, b, c$. The voltage vector V is related to the switching state S by:

$v = V_{dc}S$ [30]

where $V_{dc}$ is the DC-link voltage

## VI. PREDICTIVE DIRECT CONTROL METHODS FOR SRM

### A. Predictive Control of Current (P Current Control)
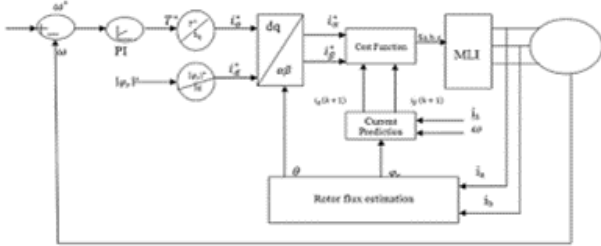


**Fig. 3 P Current Control**

Predictive Using only the expected stator currents in the set reference frame, current control (P CURRENT CONTROL) is used to regulate the multiphase drive. As shown in Fig. 3, current references are acquired in the rotating reference frame using an exterior PI speed control loop and a constant d-component current. These references are then mapped in the fixed reference frame and used in the cost function.Multiphase drives with various numbers of windings have been used to execute this straightforward predictive controller system [10].

Sinusoidal stator current standards in the a-b-c phase coordinates are necessary to generate the appropriate electric power. The control objective is transformed into either a null or non-null reference stator current vector in the x-y plane, depending on the multiphase machine used. The reference stator current vector in the - plane is constant in amplitude but varies its electrical angle in a circular trajectory. MPC-based predictive current controller with an external speed control loop.The SRM model, stator current is as below:

$i_s = -\frac{1}{R_\sigma}\left(\left(L_\sigma \cdot \frac{di_s}{dt} - K_r \cdot \left(\frac{1}{\tau_r} - j.\omega\right).\varphi_r\right) - v_s\right)$ [31]

where$K_r = \frac{L_m}{L_r}$, $R_\sigma = R_s + K_r^2 . R_r$ and $L_\sigma = \sigma . L_s$

The forward Euler discretization is as

$\frac{dx}{dt} \cong \frac{x(k+1)-x(k)}{T_s}$ [32]

where$T_s$ is the sampling time of the system.

Using (8) and (9), the stator current can be predicted as

$\bar{\imath}_s(k+1) = \left(1 - \frac{T_s}{T_\sigma}\right).i_s(k) + \frac{T_s}{T_\sigma}.\frac{1}{R_\sigma}.\left[K_r.\left(\frac{1}{T_r} - j.\omega(k)\right).\varphi_r(k) + v_s(k)\right]$ [33]

$where\ T_\sigma = \sigma.\frac{L_s}{R_\sigma}$

The cost function is represented as below:

$g_j = \sum_{h=1}^{N}\{|i_\alpha^* - i_\alpha(k+h)_j| + |i_\beta^* - i_\beta(k+h)_j|\}$ [34]

From (11), it follows that the present reference generation is required to finish designing the P CURRENT CONTROL technique. The P CURRENT CONTROL method's block layout is illustrated in Fig. 2. A speed PI controller generates the torque reference, and the reference to rotor flux magnitude is taken to be a fixed number.

The related standard numbers for the torque- and field-producing currents$i_d^*$ and $i_q^*$ are produced by

$i_d^* = \frac{|\varphi r|^*}{L_m}$ [35],

$i_q^* = \frac{2}{3}\frac{L_r}{L_m}\frac{T^*}{|\varphi r|^*}$ [36]

In the cost function, the state's current values in $\alpha\beta$ frame are required. The inverse Park transformation is presented to satisfy this requirement as follows:

$\begin{pmatrix} \alpha \\ \beta \end{pmatrix} = \begin{pmatrix} cos(\theta) & -sin(\theta) \\ sin(\theta) & cos(\theta) \end{pmatrix}\begin{pmatrix} d \\ q \end{pmatrix}$ [37]

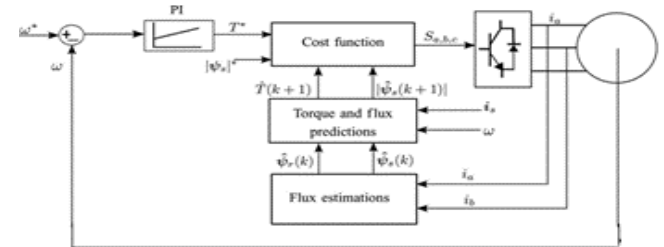### B. Predictive Control Of Torque (P Torque Control)



**Fig. 4 MPC based Predictive Controller of Torque with an Outer Speed Control Loop**

For three phase, two stage induction motor systems, Predictive Controller of Torque (P TORQUE CONTROL) based on FCS-MPC is shown in Fig. 4. The stator flux and torque are controlled variables, and the process is run by an internal P TORQUE CONTROL and an external PI-based speed control. The torque reference is provided by an external PI based on the speed error, while the stator flux reference is fixed to its usual value for base speed operation.After evaluating the cost function [20] [22] [24] [25] [26], the switching condition with a decreased cost (J) is then utilised with the VSI. In order to improve P TORQUE CONTROL performance, a changed cost function that aimed to not only control stator flux and produced torque but also set a maximum attainable -stator limit was provided in [17].

Torque and flow forecasts as well as the creation of a cost function are at the heart of P TORQUE CONTROL.In the predictive algorithm, the stator fluxprediction can be obtained as

$$\bar{\varphi}_s(k+1) = \varphi_s(k) + T_s.v_s(k) - R_s.T_s.i_s(k) \qquad [38]$$

The electromagnetic torque can be

$$\bar{T}(k+1) = \frac{3}{2}.p.Im\{\bar{\varphi}_s(k+1)^*.\bar{\imath}_s(k+1)\} \qquad [39]$$

The classical cost function for the P TORQUE CONTROL method is

$$g_j = \sum_{h=1}^{N}\{|T^* - \bar{T}(k+1)_j| + \lambda.|\|\varphi_s^*\| - \|\bar{\varphi}_s(k+h)_j\||\} \qquad [40]$$

## VII. RESULTS

### A. P Current Control and P Torque Control Method with SRM and IM using15-Level Inverter

A 15-level multilayer inverter was used to model P CURRENT CONTROL and P TORQUE CONTROL for a 4-pole induction machine and compare it to a 2-level voltage source inverter. 5 HP, 440V, 50Hz, and 1440 RPM are the specifications for the induction motor. The following motion parameters will be used for all simulations:

**Table. 1: Induction Motor Parameters**

| | |
|---|---|
| Resistance of stator (ohm) | 1.403 |
| Resistance of rotor (ohm) | 1.395 |
| Self Inductance of stator (H) | = 0.005839 |
| Self Inductance of rotor (H) | 0.005839 |
| Rotor Mutual Inductance      (H) | 0.2037 |
| Number of poles | = 4 |
| Inertia (kg.m^2) | 0.0005 |
| Time of Sampling | = 1 Sec |

A 15-level multilayer inverter was used to model P CURRENT CONTROL and P TORQUE CONTROL for a 4-pole SM and compare it to a 2-level voltage source inverter. The following motion parameters will be used for all simulations: Table II lists the SRM motor's characteristics. The following motion parameters will be used for all simulations:

**Table. 2: SRM Parameters**

| | |
|---|---|
| Phase resistance Stator Rs | = 4.3 |
| Arm. Inductance | = 0.0001 |
| Linkage established by magnets | = 0.05 |
| Voltage Constant | = 18.138 |
| Torque Constant | = 0.15 |
| Inertia, friction factor, pole pairs | 0.000183 |
| Friction factor | = 0.001 |
| Pole pairs | = 2 |
| Initial conditions ia,ib(A) ] | = [0,0, 0,0] |
| Sampling Time | = 1 |

For the predictive approach, it is necessary to calculate the electromagnetic tension T(k + 1) and the next-step stator flow s(k + 1). The stator flow prediction can be created by discretizing the voltage model (1) with (9) asFigures 5, 6, and 10 compare the modelling findings of the P CURRENT CONTROL method and the P TORQUE CONTROL method with IM using a 15-level inverter to those of the P CURRENT CONTROL method and the P TORQUE CONTROL method with SRM using the same inverter [10]. The images show that both techniques behave well and similarly at this stage of the procedure. The P CURRENT CONTROL technique has a slightly better current reaction, but the P TORQUE CONTROL method has fewer torque ripples than the P

CURRENT CONTROL method does. Results across the full speed spectrum are investigated in the models. The motor goes from a positive nominal speed to a negative nominal speed. The rotor current, measured speed, and measured force are all monitored throughout this dynamic process. It is obvious that the waves of the two techniques are very similar. The same exterior speed PI factors cause them to have nearly identical settling times to finish this reversal process.When compared to the P CURRENT CONTROL technique, the torque waves produced by the P TORQUE CONTROL method are marginally smaller. Based on these models, we can say that two techniques can behave well at steady states with the complete load and perform well across the entire speed range. THD minimization was the strategy used in this research to reduce transition losses. Total harmonic distortion (THD) has been precisely calculated in this research using MATLAB 2013. The recommended method performs better in terms of Total Harmonic Distortion when compared to conventional methods for speed, torque, and stator current in fleeting situations (THD).Figs. 5(a), (b), and 6(a), (b), respectively, depict the related speed, torque, and stator current reactions of the P TORQUE CONTROL and P CURRENT CONTROL systems using SRM with a 15-level converter (c). In the P CURRENT CONTROL and P TORQUE CONTROL using SRM with 15-level converter, Figures 9(a),(b),(c) and Figure 10(a),(b),(c) respectively show the THD in speed, electromagnetic torque, and stator current.Figs. 7(a), (b), and 8(a), (b), respectively, show the corresponding speed, torque, and stator current reactions of the P TORQUE CONTROL and P CURRENT CONTROL systems with a 15-level converter using IM (c). The THD in speed, electromagnetic torque, and stator current for the P CURRENT CONTROL and P TORQUE CONTROL techniques with IM using a 15-level converter are shown in Figures 11(a), (b), and 12(a), (b), respectively.According to article [10], P CURRENT CONTROL and P TORQUE CONTROL decrease THD in speed, torque, and rotor current by roughly 5.3% and 4.8%, respectively, in the conventional system. When compared to article [10] [23] shown in Table 3, the suggested P CURRENT CONTROL and P TORQUE CONTROL system with 15-level inverter is shown to be better to the standard one by the THD in speed, torque, and stator current with P CURRENT CONTROL and P TORQUE CONTROL being decreased by roughly 23% and 23%, respectively.

### B. P Current Control and P Torque Control Method with SRM and IM using2-Level Inverter

Figures 3 and 4 depict the Matlab and Simulink model of the P CURRENT CONTROL and P TORQUE CONTROL methods with SRM using a 2-level inverter. The external PI speed regulators are set up with the same settings to enable comparison between the two approaches. The simulation results of the P CURRENT CONTROL method and the P TORQUE CONTROL method with SRM using 2-level inverter is shown in fig.13(a),(b),(c) and  fig.14 (a),(b),(c) compared with the simulation results of the.

P CURRENT CONTROL method and the P TORQUE CONTROL method with IM using 2-level inverter shown in Fig.15 (a),(b),(c), Fig.16 (a),(b),(c) respectively [10]. The images show that both techniques behave well and similarly at this stage of the procedure. The P CURRENT CONTROL method has a slightly better current response; however, the torque ripples of the P TORQUE CONTROL method are lower than those of the P CURRENT CONTROL method. The performances in the whole speed range are investigated in the simulations. The motor rotates from positive nominal speed to negative nominal speed. During this dynamic process, the measured speed, the torque, and the stator current are observed. It is clear that both methods have very similar waveforms. They each have almost the same settling time to complete this reversal process due to the same external speed PI parameters. The torque ripples of the P TORQUE CONTROL method are slightly lower than those of the P CURRENT CONTROL method. From these simulations, we can conclude that two methods can work well in the whole speed range and have good behaviours with the full load at steady states.

The method used in this study to minimise switching losses is THD minimization. In this study, total harmonic distortion (THD) has been accurately computed using MATLAB 2013. The recommended method performs better in terms of Total Harmonic Distortion when compared to conventional methods for speed, torque, and stator current in fleeting situations (THD).The corresponding speed, torque, and stator current responses of the P TORQUE CONTROL and P CURRENT CONTROL systems using SRM with a 2-level converter are shown in Figs. 13 (a), (b), (c), and 14 (a), (b), (c), respectively. Figures 17(a),(b),(c) and Figure 18(a),(b),(c) respectively demonstrate the THD in speed, electromagnetic torque, and stator current in the P CURRENT CONTROL and P TORQUE CONTROL using SRM with 2-level converter. The related speed, torque, and stator current responses of the P TORQUE CONTROL and P CURRENT CONTROL systems using IM with a 2-level inverter are similarly depicted in Fig. 15(a), (b), (c), and Fig. 16(a), (b), (c).The THD in speed, electromagnetic torque, and stator current for a 2-level converter using the P CURRENT CONTROL and P TORQUE CONTROL methods are depicted in Figs. 19(a), (b), and 20(a), (b), respectively. According to article [10], P CURRENT CONTROL and P TORQUE CONTROL decrease THD in speed, torque, and rotor current by roughly 5.3% and 4.8%, respectively, in the conventional system. The THD in speed, torque, and when stator current with P CURRENT CONTROL and P TORQUE CONTROL is decreased by approximately 19% and 36%, respectively, when compared to article [10] [23] indicate that the suggested P CURRENT CONTROL and P TORQUE CONTROL system with 2-level converter is better to the standard one. The SRM method provides 10% to 30% more power than an induction motor and doesn't require a modulator, making it the most practical direct control method, along with the P TORQUE CONTROL and P CURRENT CONTROL methods [3]. With the same current, an induction motor can only generate between 70 and 90 percent of the force generated by an SRM due to its delayed power factor. In this paper, total harmonic distortion (THD) has been accurately computed using MATLAB 2013 in

comparison to (10). In comparison to the P CURRENT CONTROL and P TORQUE CONTROL method with a 15-level H-bridge multilevel inverter using an induction motor, which is detailed in Table.3 [21], the SRM method with a 15-level H-bridge multilevel inverter lowers 23% more THD in power, speed, and stator current. The graphs 1, 2, and 3 also illustrate the graphical depiction of the percentage of THD in the rotor speed, electromagnetic torque, and stator current. The table also includes comparisons of P CURRENT CONTROL and P TORQUE CONTROL's problems.4. Switching losses are kept to a minimum because transistors are only turned on when necessary to maintain the limits of torque and flux. To improve the efficiency of a multilevel converter, semiconductor switches are switched in a specific sequence. This plan improves productivity and reduces costs while reducing switching loss. When compared to P TORQUE CONTROL and P CURRENT CONTROL methods using a 2-level voltage source inverter, Direct Torque Control of Induction Motor (DTC), and Direct Torque Control of Induction Motor with Fuzzy Logic Controller, the 15-level H-bridge multilevel inverter used in this study with SRM and IM provides excellent torque and flux responses, robust, and stable operation is achieved. (DTC with fuzzy). Due to its simple formula and strong results in both stable and transient states, this innovative technique rapidly drew the attention of academics. In terms of speed, torque, and stator current ripple during transient circumstances, the suggested system responds better than the usual one [10].

Fig.5: Current Controller with 15- MLI SRM Result
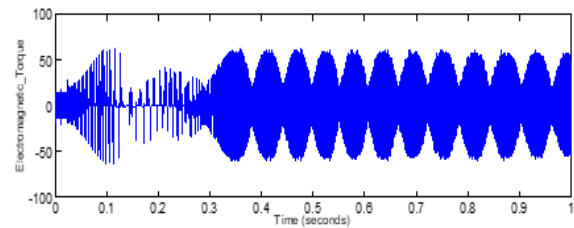


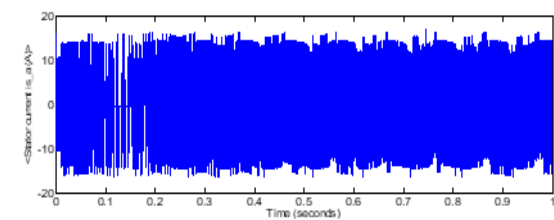**Fig. 5.(a) Electromagnetic Torque in P Current Controller**


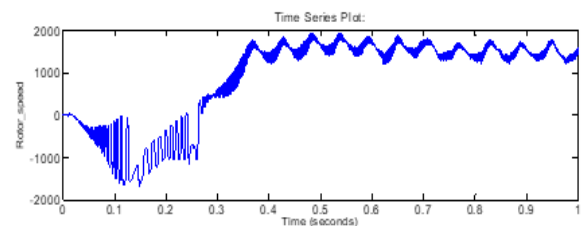
**Fig. 5.(b) Stator Current in P Current Controller**



**Fig. 5.(c) Rotor speed in P Current Controller**

32

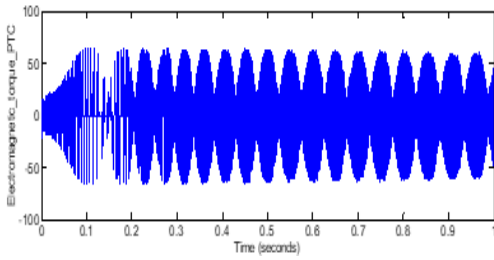Fig.6: PTorque Ccontroller with 15-MLI SRM result



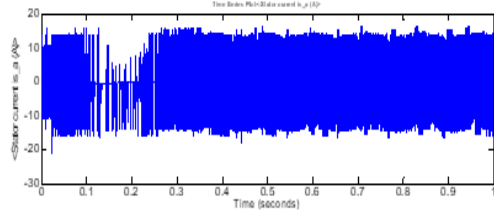**Fig. 6. (a) Electromagnetic Torque in PTorque Controller**



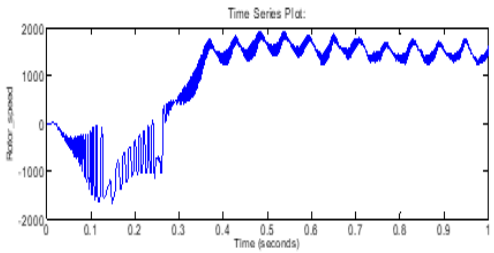**Fig. 6. (b) Stator current in PTorque Controller**



**Fig. 6. (c) Rotor speed in PTorque Controller**
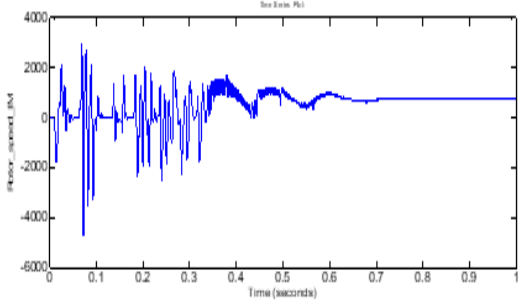
Fig.7: P P Current Controller with 15-level MLI using IM
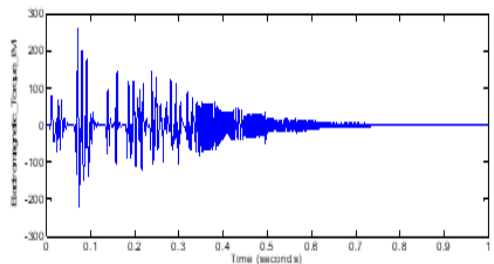


**Fig. 7. (a) Speed in P Current Controller**
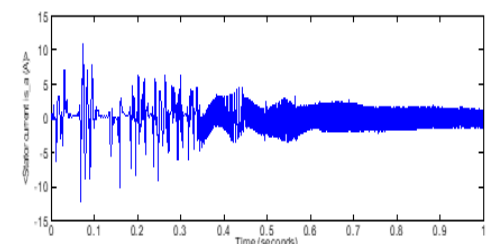


**Fig. 7. (b) Torque in P Current Controller**



**Fig. 7. (c)Current in P Current Controller Stator**
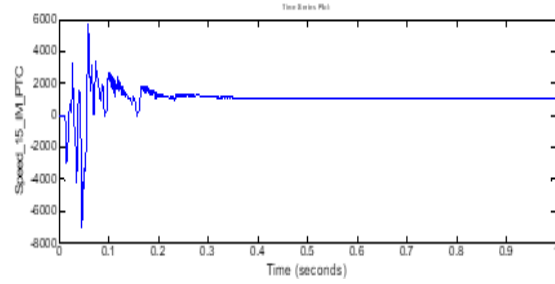
Fig.8: P TORQUE CONTROL with 15-level MLI using IM result



**Fig. 8. (a) Speed in PTorque Controller**
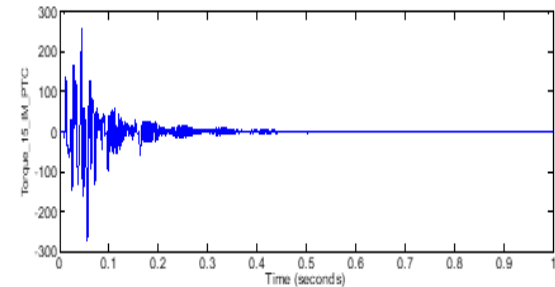


**Fig. 8. (b) Torque in PTorque Controller**
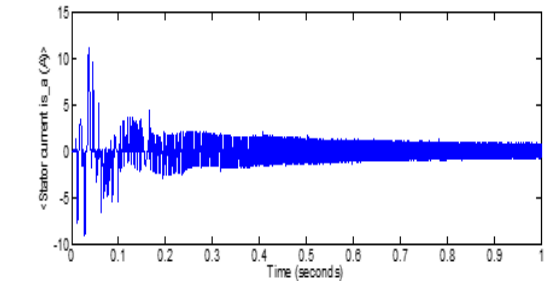


**Fig. 8. (c) Current in PTorque Controller**

Fig.9: THD in PCurrent Control with 15-level MLI using SRM result
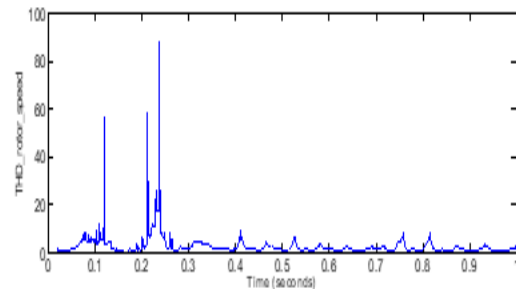


**Fig. 9. (a) Rotor Speed Consist THD**
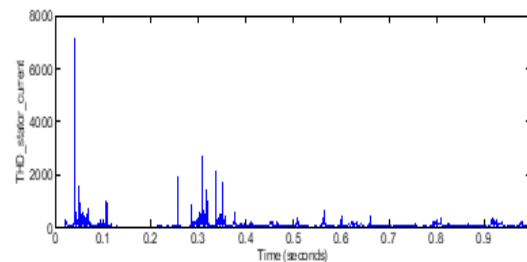


**Fig. 9. (b) Stator Current Consisit THD**
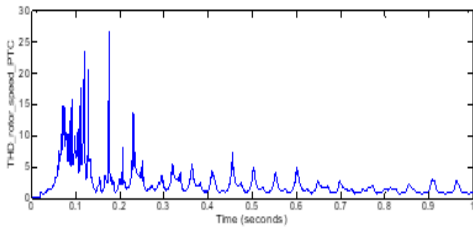
**Fig. 9. (c) Torque THD**

Fig.10: THD in P TORQUE CONTROL with 15- MLI using usingSRM
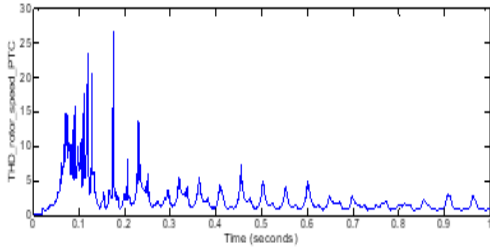


**Fig. 10. (a) Rotor Speed THD**
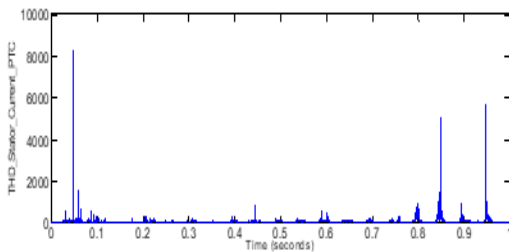


**Fig. 10. (b) Stator Current THD**
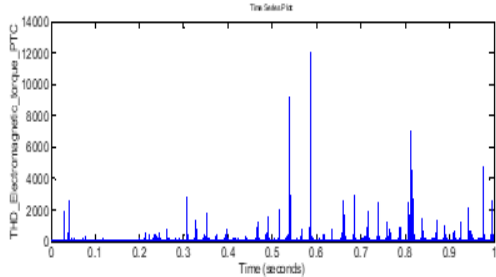


**Fig. 10. (c) Torque THD**

Fig.11: THD in PCurrent Control with 15-level MLI using IM
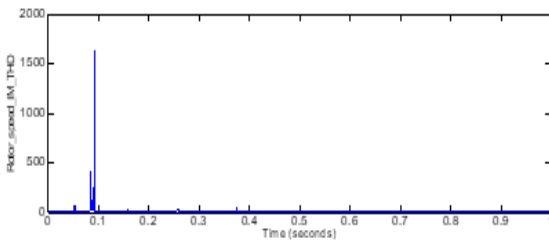


**Fig. 11.(a) Rotor Speed THD**
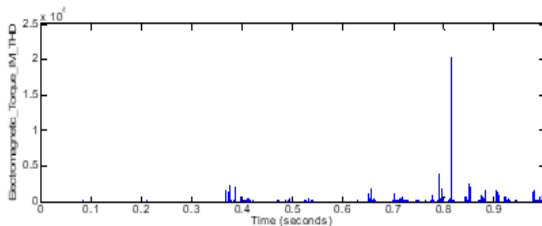


**Fig. 11.(b) Torque THD**
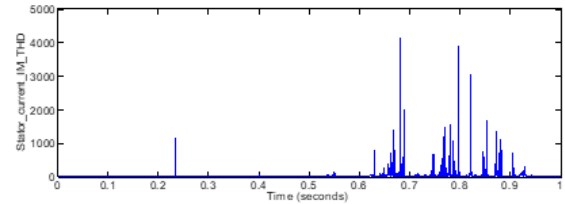


**Fig. 11.(c) Stator Current THD**

Fig.12: THD in P TORQUE CONTROL with 15- MLI using IM
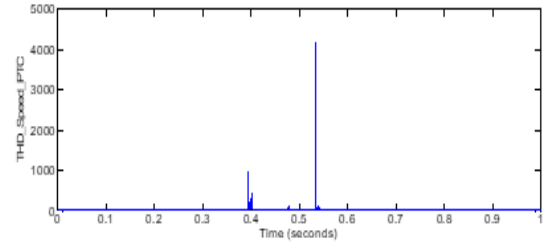


**Fig. 12. (a) Rotor Speed THD**
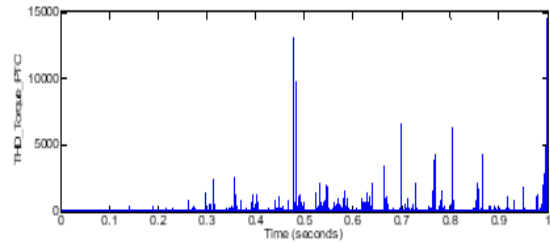


**Fig. 12. (b) Torque THD**
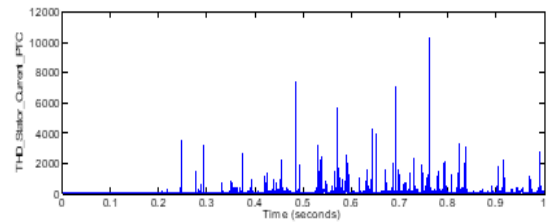


**Fig. 12. (c) Stator Current THD**

Fig.13: P Current Control with 2-level VSI using SRM
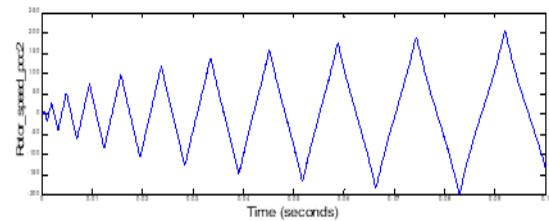


**Fig. 13 (a) Rotor speed in P Current Control**
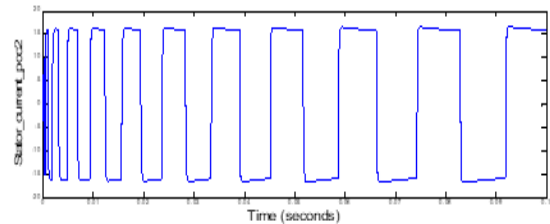


**Fig. 13 (b) Stator Current in P Current Control**

34
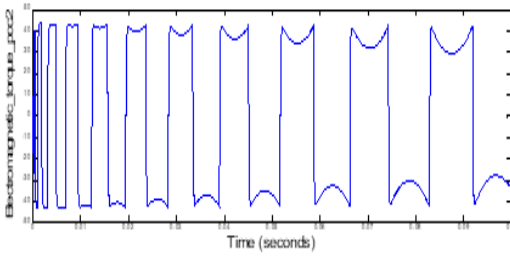
**Fig. 13 (c) Obtained Torque in P Current Control**

Fig.14: P Torque Control with 2-level VSI using SRM
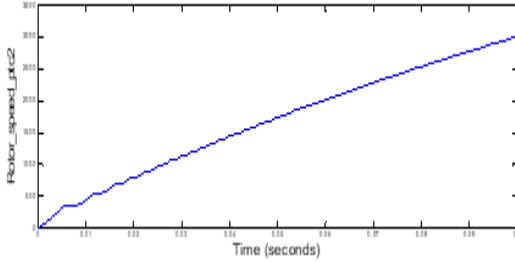


**Fig. 14 (a) Rotor Speed in P Torque Control**
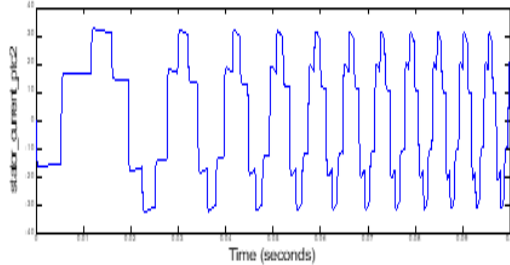


**Fig. 14 (b) Stator Current in P Torque Control**
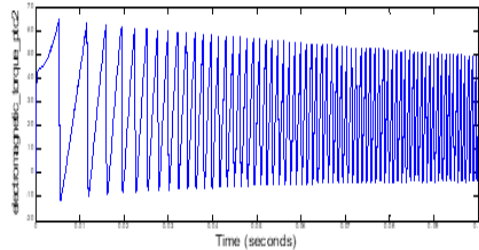


**Fig. 14 (c) Obtained Torque in P Torque Control**

Fig.15: P Current Control with 2-level VSI using IM
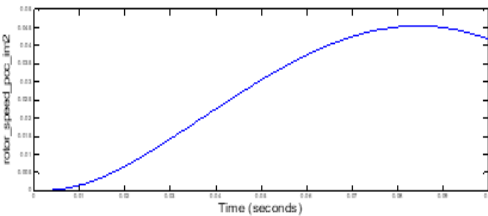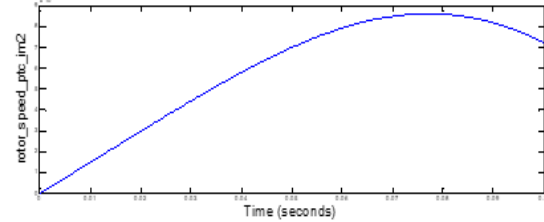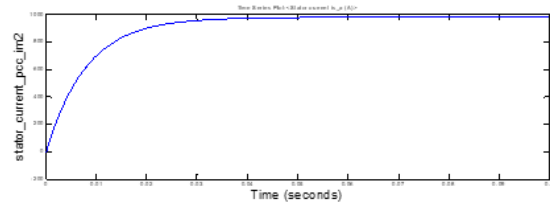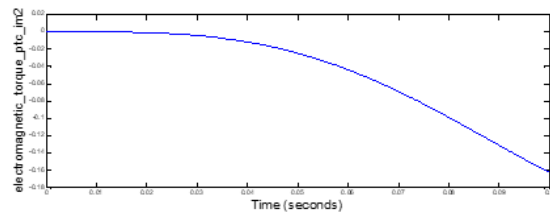


**Fig. 15 (a) Rotor Speed in P Current Control**
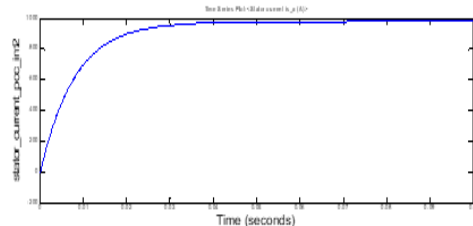


**Fig. 15 (b) Stator Current in P Current Control**
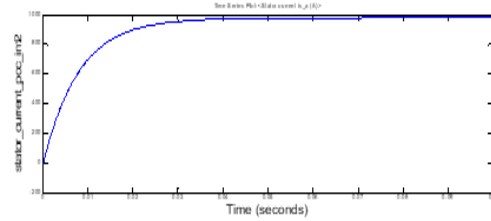


**Fig. 15(c) Obtained Torque in P Current Control**

Fig.16: P TORQUE CONTROL with 2-level VSI using IM
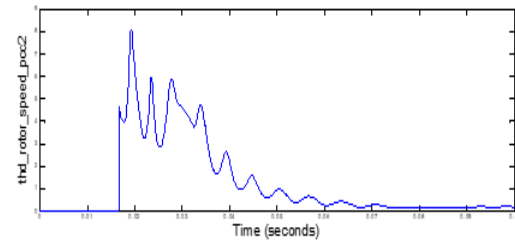


**Fig. 16 (a) Rotor Speed in P Torque Control**
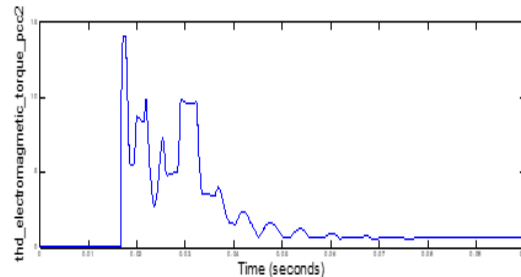


**Fig. 16 (b) Stator Current in P Torque Control**



**Fig. 16 (c) Obtained Torque in P Torque Control**

Fig.17: THD in P CURRENT CONTROL with 2-level VSI using SRM



**Fig. 17 (a) THD in Rotor Speed**
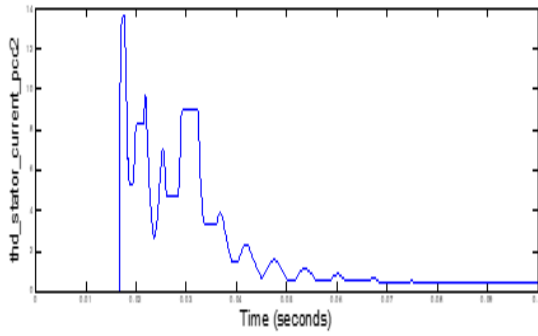


**Fig. 17 (b) THD in Electromagnetic Torque**

**Fig. 17 (c) THD in Stator Current**

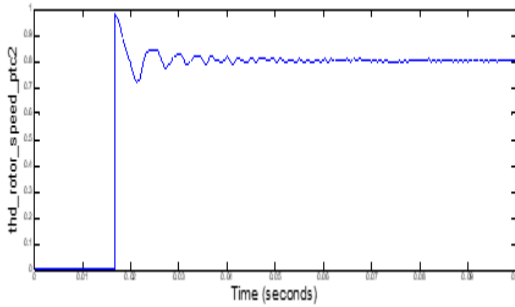Fig.18: THD in P Torque Control with 2-level VSI using SRM
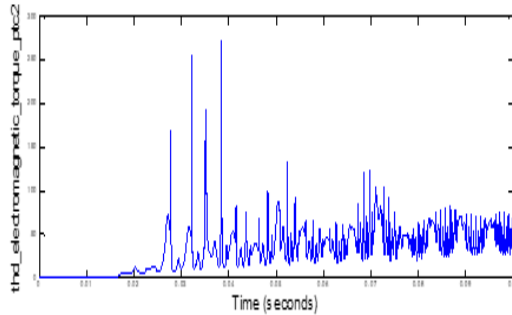


**Fig. 18 (a) THD Rotor Speed**



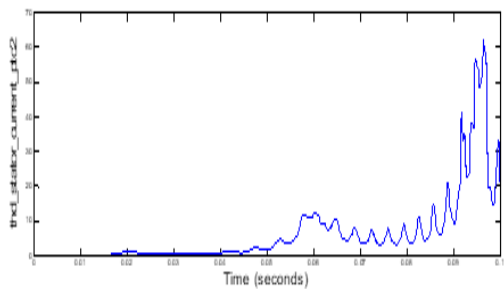**Fig. 18(b) THD Electromagnetictorque**



**Fig. 18 (c) THD Stator Current**

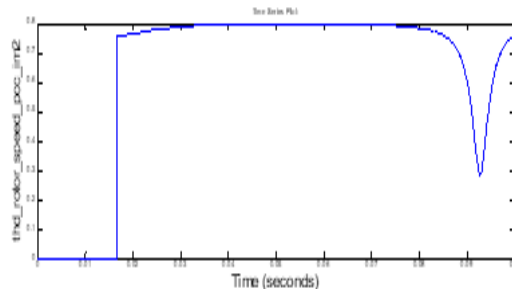Fig.19: THD in P CURRENT CONTROL with 2-level VSI using IM
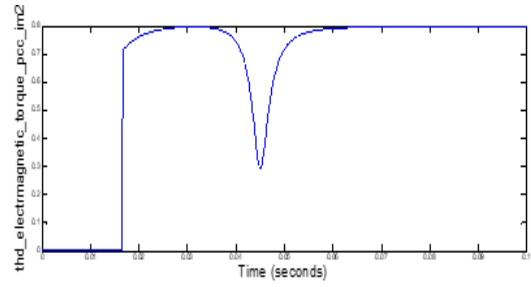


**Fig. 19 (a) THD in Rotor Speed**



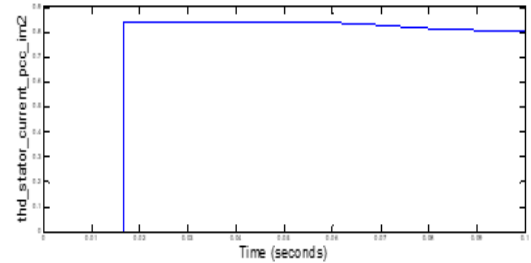**Fig. 19 (b) THD in Electromagnetic Torque**



**Fig. 19 (c) THD in Stator Current**
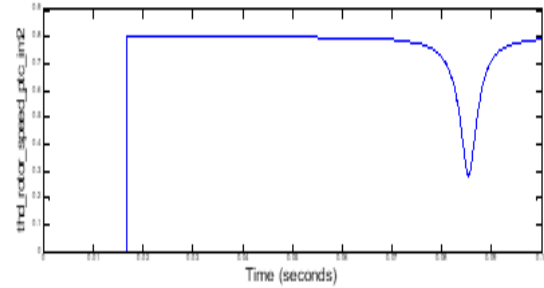
Fig.20: THD in P Torque Control with 2-level VSI using IM
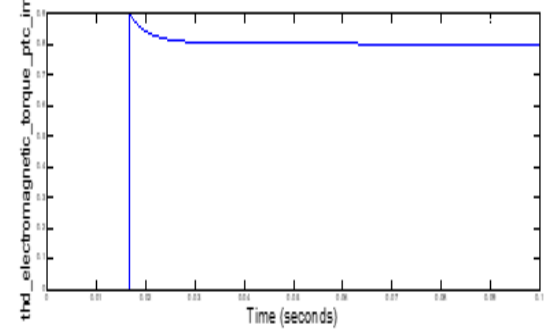


**Fig. 20 (a) THD Rotor Speed**
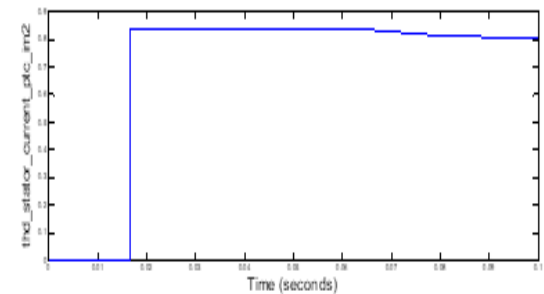


**Fig. 20 (b) THD Electromagnetic Torque**



**Fig. 20 (c) THD Stator Current**

## C. THD Analysis of P Current Control and P Torque Control Method

### Table.3: %THD Calculation Comparison

| Sr. No | Different Methods | %THD in | | |
|---|---|---|---|---|
| | | Rotor Speed ($w_r$) | Torque ($T_e$) | Stator Current |
| 1 | P CURRENT CONTROL with SRM using 15-level multilevel inverter | 31.44 | 31.34 | 44.85 |
| 2 | P TORQUE CONTROL with SRM using 15-level multilevel inverter | 21 | 21 | 118 |
| 3 | P CURRENT CONTROL with IM using 15-level multilevel inverter | 54.24 | 155.2 | 53.22 |
| 4 | P TORQUE CONTROL with IM using 15-level multilevel inverter | 41.51 | 41.51 | 89.67 |
| 5 | P CURRENT CONTROL with SRM using 2-level voltage source inverter(VSI) | 82.45 | 68.60 | 39.39 |
| 6 | P TORQUE CONTROL with SRM using 2-level voltage source inverter(VSI) | 106.11 | 41.40 | 90.02 |
| 7 | P CURRENT CONTROL with IM using 2-level voltage source inverter(VSI) | 118.86 | 98.14 | 72.21 |
| 8 | P TORQUE CONTROL with IM using 2-level voltage source inverter(VSI) | 57.20 | 79.38 | 102.34 |
| 9 | Direct Torque control of IM using 2-level voltage source inverter(VSI) | 49.53 | 81.62 | 157.84 |
| 10 | Direct Torque control of IM with Fuzzy Logic Controller using 2-level voltage source inverter(VSI) | 49.53 | 61.82 | 137.14 |

## D. Comparative Issues between P CURRENT CONTROL and P TORQUE CONTROL

### Table.4: Comparative Issues between P Current Control and P Torque Control

| Feature | P Current Control | P Torque Control |
|---|---|---|
| Conceptual Complexity | Poor | Poor |
| PI-current controller | Not Req | Not Req |
| Use of PWM | Not Req | Not Req |
| Switching Frequency | Varying | Varying |
| Dynamics | Quick | Quick |
| Torque Ripple | Higher | Lower |
| Stator current THD | Poor | Poor |
| System Constraints Inclusion | Easyly | Easyly |

## E. Graphical Representation of % THD in Speed, Torque and Stator Current
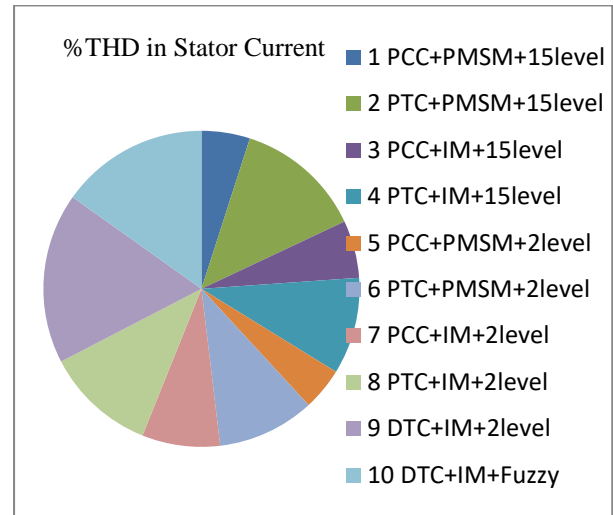


**a. Graph-1:% THD in Stator**
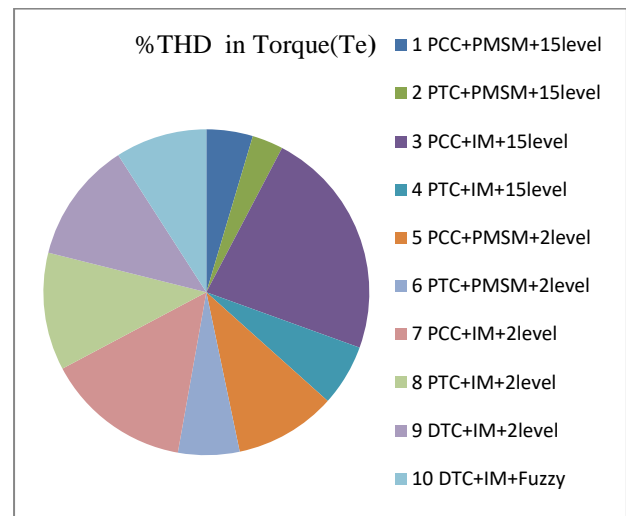


**b. Graph-1:% THD in Torque**
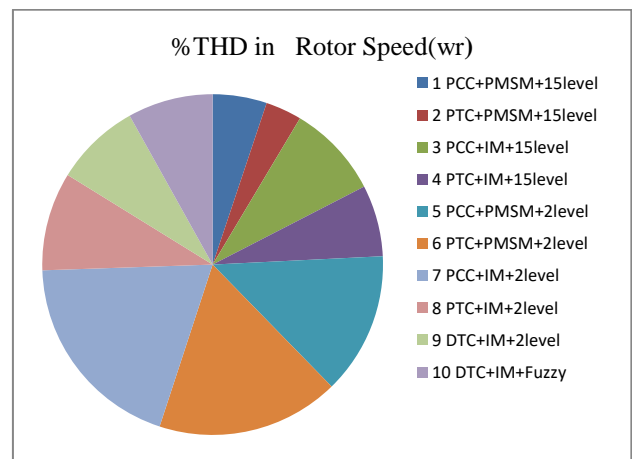


**c. Graph-1:% THD in Rotor Speed**

## VIII. CONCLUSION

This paper presents and investigates the P CURRENT CONTROL and P TORQUE CONTROL methods of the MPC family with a 15-level multilevel inverter using solely simulation methodology.

# Predictive Controller Strategies for Electrical Drives System using Inverter System

Compared to the P TORQUE CONTROL method with a 15-level multilevel inverter, the P CURRENT CONTROL method has a quicker computation time, a quicker dynamic reaction, and reduced stator current harmonics. Without an interior current PI controller or a modulator, both techniques are direct control techniques.

The P CURRENT CONTROL technique is more effective for uses with extended prediction horizons as a result of this benefit. According to the test findings, the P CURRENT CONTROL method and the P TORQUE CONTROL method with a 15-level multilevel inverter both work admirably in constant and transient conditions. The P CURRENT CONTROL method with a 15-level multilevel inverter is superior when the currents are assessed, but the P TORQUE CONTROL method with a 15-level multilayer inverter has smaller torque ripples. Due to its simple formula and strong results in both stable and transient states, this innovative technique rapidly drew the attention of academics.

Future research will evaluate switched reluctance motors, and when P CURRENT CONTROL and P TORQUE CONTROL methods are applied to servo motors with multiple inverters, we expect that the computation time will be significantly reduced. The P TORQUE CONTROL method exhibits significantly greater resilience with regard to the magnetising inductance than the P CURRENT CONTROL method does with regard to the stator resistance.

## DECLARATION STATEMENT

| | |
|---|---|
| Funding | No, I did not receive. |
| Conflicts of Interest | No conflicts of interest to the best of our knowledge. |
| Ethical Approval and Consent to Participate | No, the article does not require ethical approval and consent to participate with evidence. |
| Availability of Data and Material | Not relevant. |
| Authors Contributions | All authors have equal participation in this article. |

## REFERENCES

1. Patricio Cortés, Marian P. Kazmierkowski, and Ralph M. Kennel, Daniel E. Quevedo, and José Rodríguez, "Predictive Control in Power Electronics and Drives," IEEE Transactions On Industrial Electronics, VOL. 55, NO. 12, Dec. 2008 https://doi.org/10.1109/TIE.2008.2007480
2. GeorgiosPapafotiou, Jonas Kley, Kostas G. Papadopoulos, Patrick Bohren, and Manfred Morari, "Model Predictive Direct Torque Control—Part I: Implementation and Experimental Evaluation," IEEE Transactions On Industrial Electronics, VOL. 56, NO. 6, JUNE 2009 https://doi.org/10.1109/TIE.2008.2007032
3. GeorgiosPapafotiou, Jonas Kley, Kostas G. Papadopoulos, Patrick Bohren, and Manfred Morari, "Model Predictive Direct Torque Control—Part II: Implementation and Experimental Evaluation," IEEE Transactions On Industrial Electronics, VOL. 56, NO. 6, JUNE 2009 https://doi.org/10.1109/TIE.2008.2007032
4. Thomas Burtscher and Tobias Geyer, "Deadlock Avoidance in Model Predictive Direct Torque Control," IEEE Transactions On Industry Applications, Vol. 49, No. 5, September/October 2013. https://doi.org/10.1109/TIA.2013.2261445
5. Tobias Geyer, "Model Predictive Direct Torque Control: Derivation and Analysis of the State-Feedback Control Law," IEEE Transactions On Industry Applications, Vol. 49, No. 5, September/October 2013 https://doi.org/10.1109/TIA.2013.2262255
6. James Scoltock, Tobias Geyer and Udaya K. Madawala, "A Comparison of Model Predictive Control Schemes for MV Induction Motor Drives," IEEE Transactions On Industrial Informatics, Vol. 9, No. 2, May 2013 https://doi.org/10.1109/TII.2012.2223706
7. YongchangZhang  andHaitao Yang, "Model Predictive controller of torque of Induction Motor Drives With Optimal Duty Cycle Control," IEEE Transactions On Power Electronics, Vol. 29, No. 12, December 2014 https://doi.org/10.1109/TPEL.2014.2302838
8. Fengxiang Wang, Zhenbin Zhang, S. AlirezaDavari, Reza Fotouhi, Davood Arab Khaburi, José Rodríguez, and Ralph Kennel,  "An EncoderlessPredictive controller of torque for an Induction Machine With a Revised Prediction Model and EFOSMO," IEEE Transactions On Industrial Electronics, Vol. 61, No. 12, December 2014 https://doi.org/10.1109/TIE.2014.2317140
9. PetrosKaramanakos, , Peter Stolze, *Student Member,* Ralph M. Kennel, Stefanos Manias, and Hendrik du Toit Mouton, "Variable Switching Point Predictive controller of torque of Induction Machines," IEEE Journal Of Emerging And Selected Topics In Power Electronics, Vol. 2, No. 2, June 2014 https://doi.org/10.1109/JESTPE.2013.2296794
10. Fengxiang Wang, *Member, IEEE*, Shihua Li, *Senior Member, IEEE*, Xuezhu Mei, Wei Xie, *Member, IEEE*, José Rodríguez, *Fellow, IEEE*, and Ralph M. Kennel, *Senior Member, IEEE*, "Model-Based Predictive Direct Control Strategies for Electrical Drives: An Experimental Evaluation of P TORQUE CONTROL and P CURRENT CONTROL Methods," IEEE Transactions On Industrial Informatics, Vol. 11, No. 3, June 2015 https://doi.org/10.1109/TII.2015.2423154
11. Md. Habibullah, *Student Member, IEEE,* and Dylan Dah-Chuan Lu, *Senior Member, IEEE*, "A Speed-Sensorless FS-P TORQUE CONTROL of Induction Motors Using Extended Kalman Filters," IEEE Transactions On Industrial Electronics, Vol. 11, No. 3, Aug 2015 https://doi.org/10.1109/TIE.2015.2442525
12. Takahashi and T. Noguchi, "A new quick-response and high-efficiency control strategy of an induction motor," IEEE Trans. Ind. Appl., vol. 22, no. 5, pp. 820–827, Sep. 1986. https://doi.org/10.1109/TIA.1986.4504799
13. I. Takahashi and Y. Ohmori, "High-performance direct torque control of an induction motor," IEEE Trans. Ind. Appl., vol. 25, no. 2, pp. 257–264, Mar./Apr. 1989. https://doi.org/10.1109/28.25540
14. M. Morari and J. Lee, "Model predictive control: Past, present and future," Comput. Chem. Eng., vol. 23, no. 4, pp. 667–682, 1999. https://doi.org/10.1016/S0098-1354(98)00301-9
15. J. Holtz and S. Stadtfeldt, "A predictive controller for the stator current vector of AC machines fed from a switched voltage source," in Proc. IEEE Int. Power Electron. Conf. (IPEC), Mar. 27–31, 1983, vol. 2, pp. 1665–1675.
16. R. Kennel and D. Schöder, "A predictive control strategy for converters," in Proc. IFAC Control Power Electron. Elect. Drives, 1983, pp. 415–422. https://doi.org/10.1016/B978-0-08-030536-3.50061-1
17. M. Preindl and S. Bolognani, "Model predictive direct torque control with finite control set for SRM drive systems, part 1: Maximum torque per ampere operation," IEEE Trans. Ind. Informat., vol. 9, no. 4, pp. 1912–1921, Nov. 2013. https://doi.org/10.1109/TII.2012.2227265
18. M. Preindl and S. Bolognani, "Model predictive direct torque control with finite control set for SRM drive systems, part 2: Field weakening operation," IEEE Trans. Ind. Informat., vol. 9, no. 2, pp. 648–657, May 2013. https://doi.org/10.1109/TII.2012.2220353
19. C. Rojas et al., "Predictive torque and flux control without weighting factors," IEEE Trans. Ind. Electron., vol. 60, no. 2, pp. 681–690, Feb. 2013. https://doi.org/10.1109/TIE.2012.2206344
20. J. Rodriguez *et al.*, "State of the art of finite control set model predictive control in power electronics," *IEEE Trans. Ind. Informat.*, vol. 9, no. 2, pp. 1003–1016, May 2013. [17] J. Rodriguez *et al.*, "Predictive controller of current of a voltage source inverter," *IEEE Trans. Ind. Electron.*, vol. 54, no. 1, pp. 495–503, Feb. 2007. https://doi.org/10.1109/TIE.2006.888802
21. SurajKarpe,    Sanjay.A.Deokar,AratiM.Dixit,""Switching    losses minimization and performance improvement of P CURRENT CONTROL and P TORQUE CONTROL methods of model predictive direct torque control drives with 15-level inverter",JESIT ,vol.1,December 2017. https://doi.org/10.1016/j.jesit.2017.01.009
22. SurajKarpe, Sanjay.A.Deokar,Ulhas B. Shinde,"Improved Performance of Direct Torque Control with PMSM compared to DTC with Induction Motor",TURCOMAT ,vol.1,December 2017.
23. SurajKarpe,    Sanjay.A.Deokar,AratiM.Dixit,"Switching    Losses Minimization by Direct Torque Control,"JESIT ,vol.12,December 2021.

38

24. Reddy, B. E., Praveen, J., & Kumar A, V. (2019). Implementation of DSP Based Voltage Source Inverter (VSI) by using Sinusoidal Pulse Width Modulation Technique. In International Journal of Recent Technology and Engineering (IJRTE) (Vol. 8, Issue 2, pp. 4176–4180). https://doi.org/10.35940/ijrte.b3262.078219

25. Sharma, A. K. (2019). Simulation Implementation of Three Phase VSI Fed Three Phase Induction Motor Drive with Filter. In International Journal of Engineering and Advanced Technology (Vol. 8, Issue 6, pp. 1462–1468). https://doi.org/10.35940/ijeat.f8126.088619

26. Deepak, F. X. E., Senthamil, L. S., Umamaheswari, S., Nicholine, J. P., & Rathish, R. J. (2019). Fuzzy Logic Controlled PV Based Quasi Impedance Source Inverter for Charge Balancing. In International Journal of Innovative Technology and Exploring Engineering (Vol. 9, Issue 1, pp. 2633–2638). https://doi.org/10.35940/ijitee.a5338.119119

27. ALAHMAD, A. (2023). Using Medium Voltage Variable Frequency Drives Instead of Medium Voltage Switchgear in a Pump System. In Indian Journal of Signal Processing (Vol. 3, Issue 1, pp. 1–5). https://doi.org/10.54105/ijsp.b1014.023123

28. Paliwal, S., & Kalyan, B. S. (2022). Driver's Activity Detection System using Human antenna. In Indian Journal of Energy and Energy Resources (Vol. 1, Issue 3, pp. 4–6). https://doi.org/10.54105/ijeer.c1007.051322

## AUTHORS PROFILE

**Suraj R. Karpe**, Ph.D. in Electrical Machines and Drives from SPPU Pune, in 2019. Intrest of research topic is Switching Losses Minimization and performance improvement of Induction Motor

**Sanjay Deokar,** Ph.D. in Power quality of Electrical disturbances from Nanded, Dr.Babasaheb Ambedkar Marathwada University in 2016. Intrest of research topic is Mitigation of all power quality disturbances in power system

**Dr. Ulhas B. Shinde,** working as a Principal since 2013 at CSMSS, Chh. Shahu College of Engineering, Aurangabad. Planning and Execution of Academic and Non-Academic Activities. Overall administration of institute having student strength more than 2000 and staff strength 150. Providing Guidance and Mentoring to HODs, Staff and Students of all Departments. Monitoring and providing guidance to members preparing proposals, documents related with AICTE, DTE, University, Shikshan Shulka Samiti, Admission Regulating Authority work. Continuous monitoring of activities of NBA, NAAC, and NIRF carried out by departments. Established Strong Institute Industry Relations and associated with organizations like CMIA, MASIA, BOAT, CII etc.